Biophysical Chemistry 328 (2026) 107532

Contents lists available at ScienceDirect

Biophysical Chemistry

journal homepage: www.elsevier.com/locate/biophyschem

Antimicrobial peptide mechanism of action on *S. aureus* membranes determined by *in vivo* solid-state NMR

Laila Zaatouf, Thierry Drujon, Astrid Walrant, Emmanuelle Sachon, Dror E. Warschawski *

Chimie Physique et Chimie du Vivant, CPCV, CNRS UMR 8228, Sorbonne Université, École Normale Supérieure, PSL University, 75005 Paris, France

ARTICLE INFO

Keywords:
Antimicrobial peptides
Bacteria
Lipids
Mechanism
Solid-state NMR

ABSTRACT

Staphylococcus aureus (S. aureus) is a Gram-positive pathogenic bacterium and a major cause of nosocomial infections. Between 20 % and 50 % of *S. aureus* strains are resistant to a wide range of antibiotics. DMS-DA6-NH_2 (DA6) is a novel antimicrobial peptide (AMP) that exhibits high efficacy against various bacterial strains, particularly *S. aureus*, by disrupting its membrane through an as-yet-unknown mechanism. We employed *in vivo* ^{2}H solid state Nuclear Magnetic Resonance (NMR) to investigate the mode of action of AMPs on deuterated bacteria. This technique provides insights into membrane order and its changes with increasing AMP concentration. Our results enabled us to compare the mechanism of DA6 with those of AMPs with established modes of action. We found that DA6 induces pore formation in the membrane of *S. aureus*. This protocol serves as a template for determining the mechanisms of action of other peptides, an essential step for developing and patenting such drugs for the treatment of human diseases.

1. Introduction

The interest of scientists in determining the structure of bacterial macromolecules is often driven by the goal of identifying their vulnerabilities, which can facilitate their eradication when they are responsible for diseases. One well-known vulnerability of bacteria is their membranes, and a notable class of molecules that target bacterial membranes are lytic antimicrobial peptides (AMPs), which are considered promising alternatives to traditional antibiotics for combating bacterial infections. However, a critical bottleneck for advancing these molecules to the drug market is the precise determination of their mechanism of action.

Several models have been proposed to explain how peptides disrupt membranes. These typically involve initial peptide binding to the membrane, followed either by rapid and complete membrane disruption (the "carpet" effect), or by a more gradual process involving the formation of more structurally-defined pores of various shapes. While many experimental approaches can detect membrane destruction, and some can identify pore formation, few methods are capable of monitoring the fate of the membrane across a range of peptide concentrations. Since 2012, several teams across the world have shown the potential of *in vivo* solid-state Nuclear Magnetic Resonance (NMR) on labeled bacterial membranes, to track changes in membrane order and how these changes correlate with peptides known to act *via* carpet or pore-forming mechanisms [1–11].

In the present study, we aim to extend this approach to a new and promising antimicrobial peptide, from the Dermaseptin family, isolated from the skin of the Mexican frog *Pachymedusa dacnicolor*, known as DMS-DA6. The two versions of the peptides, with a carboxamide or a carboxylic function at the *C*-terminus of the peptide, DMS-DA6-NH_2 and DMS-DA6-OH, respectively, have previously been studied and compared by [12], who determined their structures to be α-helical, and assessed their antimicrobial, hemolytical and cytotoxic activities. DMS-DA6-NH_2 has demonstrated efficacy against Gram(+) bacteria and interacts with bacterial membrane mimics, but its precise mechanism of action remains unclear.

We have investigated the effect of DMS-DA6-NH_2 on Gram(+) bacteria *Staphylococcus aureus via in vivo* solid-state NMR, and compared its activity to that of peptides aurein 1.2 and caerin 1.1 which are known to kill bacteria through a carpet mechanism and pore mechanism respectively [3]. Additionally, we have refined the experimental protocol, and introduced the concept of high-density minimum bactericidal concentration (MBC_{HD}), which is essential for this type of analysis. Our study enabled us to propose a molecular mode of action for each peptide/bacteria interaction. We anticipate that this protocol will be applicable to the study of other molecules interacting with the membranes of

* Corresponding author.
E-mail address: dror.warschawski@sorbonne-universite.fr (D.E. Warschawski).

https://doi.org/10.1016/j.bpc.2025.107532
Received 21 August 2025; Received in revised form 23 September 2025; Accepted 23 September 2025
Available online 24 September 2025

various micro-organisms.

2. Material and methods

2.1. Peptides

Three peptides were used in this study: aurein 1.2-NH_2 (GLFDIIK-KIAESF-NH_2, MM = 1478.85 Da, charge +1 at pH 7), also called aurein, caerin 1.1-NH_2 (GLLSVLGSVAKHVLPHVVPVIAEHL-NH_2, MM = 2582.54 Da, charge +1 at pH 7), also called caerin, and DMS-DA6-NH_2 (GVWGIAKIAGKVLGNILPHVFSSNQS-NH_2, MM = 2690.5 Da, charge +3 at pH 7), also called DA6 in this study. While they originate from the skin of various frogs, they were all synthesized by the protein engineering facility of IBPS (Sorbonne Université, Paris, France). Peptides are purified as trifluoroacetate salts, and purity is >95 % based on HPLC and mass spectrometry.

2.2. Bacterial culture

Solutions of 2 mM deuterated palmitic acid (PA-d_{31}) with polyoxyethylenesorbitan monolaurate (Tween 20) at 5 mM in 8 mL of Lysogeny Broth (LB) medium were prepared [13–14]. PA-d_{31} and Tween 20 were purchased from Avanti/Merck (St-Quentin-en-Yvelines, France). Bacteria used in this study are *Staphylococcus aureus* ATCC 6538. *S. aureus* bacteria were grown in 300 mL LB at 24 °C, shaking at 200 rpm. After 90 m, the optical density at 600 nm (OD) went from 0.1 to 0.15, and 8 mL of the 2 mM PA-d_{31} solution were added to the culture, resulting in 50 μM PA-d_{31} in the medium. Cultures were stopped at the late-log phase, after 16 h for *S. aureus*, reaching an OD of *ca.* 4. Each condition has been repeated at least three times.

2.3. Lipidomics

Bacterial lipid profiles were determined by ^{31}P solution NMR and GC/MS after lipid extraction, as described in [13–14].

2.4. Peptides biological activity

The biological activity of peptides on bacteria is usually characterized by their minimal inhibitory concentration (MIC), minimal bactericidal concentration (MBC), and time to kill 99.9 % of bacteria (TK99), determined by standard procedures [15]. Biological activity was determined with *S. aureus* grown in 3 mL Mueller-Hinton (MH) medium at 37 °C, shaking at 200 rpm stopped at the mid-log phase. MIC and TK99 were determined on bacteria at an OD of 0.003 (5×10^5 CFU/mL). TK99 was determined for a peptide concentration of twice the MIC, and aliquots are taken every 10 min. The MIC value was determined by measuring the OD on a microplate reader (POLARstar Optima, BMG, Champigny s/Marne, France) after incubation at 37 °C overnight. MBC and TK99 were determined by counting CFU (colony forming unit) on Petri dishes, after incubation for 24 h at 37 °C.

2.5. Sample preparation for solid-state NMR

Solutions of antimicrobial peptides at various concentrations (see **Table S1**) were prepared in 3 mL of isotonic solution (0.85 % NaCl). Note that the highly concentrated solutions can use up to 5 mg of peptide. When the culture was stopped (OD *ca.* 4), five aliquots of culture were collected, corresponding to a wet pellet that will fit the solid-state NMR rotor (around 50 mg, 9 mL culture for an OD of 4). Each aliquot was pelleted (4000 g for 10 min, at 4 °C), and washed twice with 5 mL of cold isotonic solution, to remove all remaining detergent molecules in solution *and* in the membrane. 200 mL of culture were left and could be used for lipidomics.

One pellet was then resuspended either with 3 mL of isotonic solution (negative control), 1 mL of 10 % formaldehyde solution (positive control), or 3 mL of antimicrobial peptide solution, while the other pellets were left at 4 °C. The first pellet was then exposed for one hour, at 37 °C under agitation. Note that during the exposition, the bacterial culture was concentrated to an OD of *ca.* 12. Peptide properties determined by solid-state NMR therefore correspond to peptide activity at such high bacterial density conditions. The last wash was performed with 5 mL of cold *deuterium-depleted* isotonic solution, in order to remove excess peptide and the water natural-abundance deuterium signal, and the wet pellet was transferred to the solid-state NMR rotor. Note that the OD in the rotor is *ca.* 1000, but this is not the bacterial density at which the peptide is monitored.

2.6. NMR

^2H solid-state NMR was performed on a Bruker Avance III 500 wide bore spectrometer (Wissembourg, France), operating at a frequency of 76.8 MHz for ^2H, and equipped with a 4-mm magic-angle spinning (MAS) triple-resonance probe. A 10 kHz MAS frequency was used for all experiments. Spectra were recorded at 30 °C, with a Hahn echo sequence using a 100 μs delay (one rotor period) and 0.5 s recycle delay. A typical spectrum was acquired with 6 k scans, and a spectral width of 500 kHz, for about 1 h. Without any peptide or formaldehyde, at the end of this acquisition, over 70 % of bacteria are still alive. Spectra were processed using a 100 Hz exponential multiplication.

Spectral moments were determined as described by Warnet et al. [16], with the MestRenova software V14.2 (Mestrelab Research, Santiago de Compostela, Spain), using Eq. (1), where ω_r is the angular spinning frequency, N is the side band number, and A_N is the area of each sideband obtained by spectral integration.

$$M_2 = \omega_r^2 \frac{\Sigma_{N=0}^{\infty} N^2 A_N}{\Sigma_{N=0}^{\infty} A_N} \quad (1)$$

3. Results

3.1. Lipidomics

In order to optimize membrane labeling, the lipid profile of *S. aureus* was determined by ^{31}P solution NMR and GC/MS after lipid extraction. The phospholipid composition of *S. aureus* membranes was determined to be 82 % phosphatidylglycerol (PG), 4 % cardiolipin (CL) and 14 % lysyl-phosphatidylglycerol (LPG) (**Table S2**). As in *B. subtilis* [13], an additional peak appeared at −0.45 ppm on the ^{31}P solution NMR spectra (with PG at +0.65 ppm), which corresponds to an undetermined species (see **Fig. S1**). If this species contained one phosphorus per molecule, it could amount to 5 % of the molecules in the lipid extract. With 50 μM exogenous PA-d_{31} micellized in Tween 20, PG was reduced to 73 %, LPG increased to 22 % and the amount of the undetermined molecule increasing as well, to 8 %. The fatty acid composition was also determined and is given as supplementary material (**Table S3**). It showed a majority of Anteiso-C15:0 (57 %) and Anteiso-C17:0 (12 %). The absence of C12:0 confirms the removal of Tween 20 detergent molecules from the samples. With 50 μM exogenous PA-d_{31} micellized in Tween 20, Anteiso-C17:0 almost disappeared, and Anteiso-C15:0 was reduced to 29 % of the fatty acids, while 38 % of the fatty acids were PA-d_{31}, and remained as free fatty acids in the membrane (passive labeling [14]).

3.2. Peptide biological activity

The biological activities of the three peptides were characterized (see Table 1). Activity depends on the bacteria, because it may depend on their size, shape, nature and charge of lipids or cell wall, but also on their state (planktonic or in a biofilm) *etc.* and a robust protocol must be used to compare those parameters in comparable conditions, usually at 5×10^5 colony-forming unit cells per mL in a Mueller–Hinton (MH) growth medium [15]. Because bacteria have different individual physical

Table 1
Biological activities of peptides on *S. aureus* bacteria. Minimal inhibitory concentration (MIC), minimal bactericidal concentration (MBC), minimal bactericidal concentration at high density of bacteria (MBC_{HD}), time to kill 99.9 % of bacteria (TK99). Each measurement has been repeated three times. MBC_{HD} is deduced from solid-state NMR experiments (see below).

	Caerin (known pore-forming)	Aurein (known carpet)	**DA6**
MIC (μM)	10	34	1.6
MBC (μM)	20	34	1.6
MBC_{HD} (μM)	620	850	16
TK99 (min)	20	20	60

characteristics, we have verified that such concentration of bacteria corresponds to an OD 0.003 for *S. aureus* ATCC 6538. TK99 is determined at a peptide concentration of 2xMIC. Table 1 shows the promising characteristics of DA6, with very low MIC and MBC. Surprisingly, this low MIC is accompanied by a longer TK99 compared to caerin and aurein, showing that the lytic effect is independent of the time it takes for the peptide to reach the membrane.

While these classical conditions are necessary to compare the merits of peptides across different laboratories, they are not necessarily ideal in other contexts. For example, in the case of a bacterial infections or biofilms, the local concentration of bacteria is much higher and can exceed 10^8 CFU/mL in intra-abdominal abscesses [17] and reach 10^9–10^{12} CFU/mL in lungs [18], corresponding to an OD of 10 to 10,000! In addition, it is known as the "Inoculum Effect" that minimum inhibitory concentration increases, although not linearly, with bacterial concentration [19–22]. In the case of a solid-state NMR study where high bacterial concentration is also required, the minimum inhibitory and bactericidal concentrations are also different. In our study, we had to expose the peptides to bacteria at an OD of 12 (around 2×10^9 CFU/mL), and we therefore searched for peptide concentrations at which bacteria would be killed in these conditions. We called it MBC_{HD} for minimal bactericidal concentration at high density of bacteria.

One can evaluate the approximate peptide/bacteria and peptide/lipid ratios around the MBC. In the classical conditions, 5×10^5 CFU/mL of bacteria are exposed to 1 to 30 μM peptides, corresponding to a ratio of 10^{10} peptides per bacteria, or 100 to 1000 peptides per lipid (Roversi et al. [23] estimate the number of lipids per bacterium to about 4×10^7 lipids). At an OD of 12.5×10^9 CFU/mL, bacteria were exposed to 15 to 1000 μM peptides, corresponding to a ratio of 10^8 peptides per bacteria, or 1 to 10 peptides per lipid. An explanation is given by Jepson et al. [19], where cells aggregates at high densities could allow peptides to affect several cells simultaneously. *In vivo* solid-state NMR will then be studied on bacteria with peptides around MBC_{HD}.

3.3. Solid-state NMR protocol

While ^2H solid-state NMR has been used for decades to probe membrane rigidity and lipid order in artificial membranes, it has only recently been applied to living cells to follow the effect of interacting molecules, including antimicrobial peptides. It requires the deuteration of membrane molecules, either through deuterated lipids or deuterated fatty acids inserted in the membrane. We have recently shown that both labeling approaches had their pros and cons, and in the present study we use the fatty acid labeling approach, using deuterated palmitic acid (PA-d_{31}) delivered by Tween 20 micelles [14], with bacteria collected at the end of the exponential phase. Our main objective is to correlate the bacterial membrane order variation with the amount of peptide exposed. The membrane order of such bacteria is increased by the presence of palmitic acid, but it will be reduced upon peptide interaction, and we will be able to monitor this variation.

Although all the results presented here are the average of at least three experiments, reproducibility is an issue, and we have noticed that two identical labeled bacterial cultures could provide different NMR spectra, corresponding to different initial order parameters. On the other hand, the effect of an antimicrobial peptide on such bacterial order parameters was similar qualitatively. We have therefore optimized a protocol allowing for the best possible reproducibility, by performing all experiments on the same initial bacterial culture. Deuterated bacteria were grown overnight in 300 mL of growth medium with the end of the exponential phase (OD = 4) reached in the morning. Five aliquots of 9 mL were pelleted, and the rest of the culture was used for lipidomics. Each pellet was resuspended in 3 mL of buffer (OD = 12), one control, three with growing concentrations of peptide, and one with 10 % formaldehyde. They were left to incubate for one hour, at 37 °C under agitation, during which the lytic activity of the peptides occurred. Samples were pelleted again, to wash the excess of peptides that have not interacted with bacterial membranes, and the 50 mg wet pellet was then used for solid-state NMR. Each ^2H solid-state NMR experiment lasted one hour, for a total of 5 h. Eventually, the pellets could be used for a cell viability test, to correlate the molecular effect with the cellular effect.

In order to be able to make all measurements the same day, we had to limit the NMR experimental time to one hour at most, compromising on the signal/noise ratio. This requirement makes magic-angle spinning (MAS) an essential tool, reducing the experimental time from 16 h to 1 h, compared to static solid-state NMR [16]. As already noted, bacteria fully survive a one-hour experiment, even at 10 kHz MAS. Solid-state NMR provides a curve of the second spectral moment M_2, as a function of peptide concentration, which is proportional to the fatty acid order parameter in the membrane, and has been shown to be proportional to membrane order [24]. This dose response curve thereby reflects the effect of the peptide on the bacterial membrane order at the end of the incubation time. With this approach, it is possible to differentiate a carpet effect from a pore-forming effect. We confirmed the results obtained with two peptides of known mechanisms, aurein and caerin and we determined the as yet unknown mechanism of DA6, on the same bacteria.

3.4. Peptide activity by ^2H in vivo solid-state NMR

3.4.1. Caerin activity

Caerin is known for its lytic pore-forming mechanism. It has been confirmed by ^2H *in vivo* solid-state NMR on *B. subtilis*, by Laadhari et al. [3]. In the present study, we have applied our optimized protocol to study its effect on *S. aureus* bacterial membranes. Without any peptide, *S. aureus* was characterized by an M_2 of $26 \times 10^9 s^{-2}$. With increasing caerin concentration, M_2 decreased linearly down to a very low value of $1 \times 10^9 s^{-2}$. By fitting this activity curve to a straight line, the 0 intercept was reached at 620 μM of caerin, that we can call MBC_{HD} and that we report in Table 1. NMR spectra and M_2 values as a function of peptide concentration are reported on Fig. 1.

3.4.2. Aurein activity

Aurein is known for its lytic carpet mechanism. It has also been confirmed by ^2H *in vivo* solid-state NMR on *B. subtilis*, by Laadhari et al. [3]. We have applied our optimized protocol to study its effect on *S. aureus* bacterial membranes. Without any peptide, *S. aureus* was characterized by an M_2 of $23 \times 10^9 s^{-2}$ (5). This value is different from the one when studying caerin (see above, $M_2 = 26 \times 10^9 s^{-2}$), indicating a lack of labeling reproducibility, and explaining the large error bars. We note, however, that whatever the initial M_2 value, the activity curve is the same, with similar slopes. Because the initial M_2 value is that of an unaffected bacterial membrane, and hence almost constant, the slope is determined by the MBC, and therefore mostly reflects the peptide efficacy, rather than its mechanism. This reinforces the necessity to perform all experiments the same day, on the same preparation, as we do in our protocol. With aurein concentrations of 200 μM and 400 μM, M_2 increased to 31×10^9 s^{-2} and 33×10^9 s^{-2}, then decreased abruptly, reaching the MBC_{HD} at 850 μM (Fig. 2). Here, the decreasing slope is

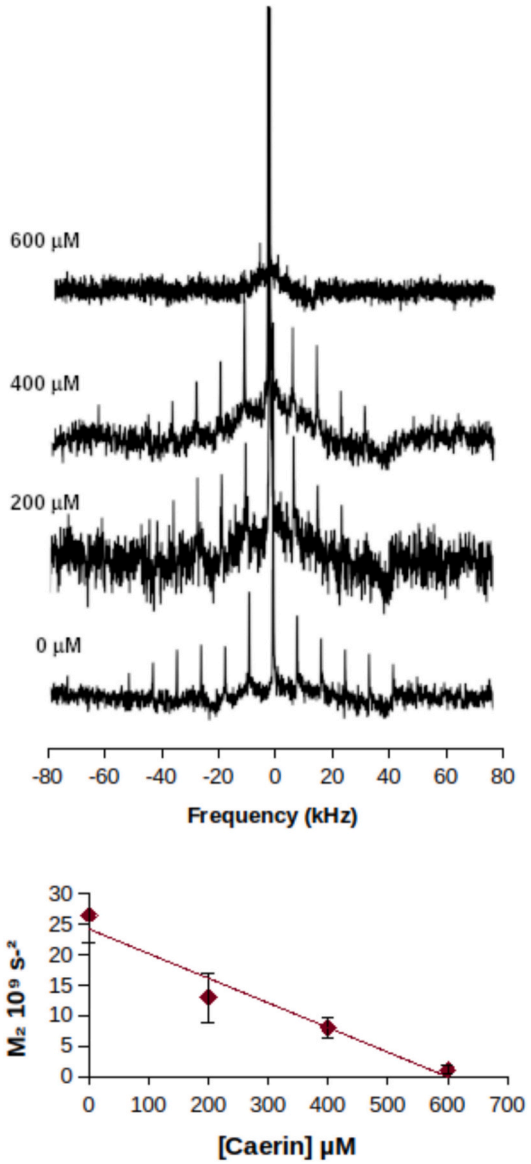

Fig. 1. (top) ^{2}H *in vivo* solid-state NMR spectra of deuterated *S. aureus* with various concentrations of caerin (the central peak is truncated). (bottom) M_2 as a function of caerin concentration, representing the activity curve of caerin on *S. aureus*. All spectra were processed using a 100 Hz exponential multiplication. Each measurement has been repeated three times. The slope of the fitting line is $-4.1 \times 10^{7}s^{-2}.\mu M^{-1}$, with an intercept at $MBC_{HD} = 620$ µM.

much larger than the increasing slope ($-7.7 \times 10^{7}s^{-2}.\mu M^{-1}$ *vs.* $2.5 \times 10^{7}s^{-2}.\mu M^{-1}$).

3.4.3. DA6 activity

DA6 is a lytic antimicrobial peptide of unknown mechanism. We have applied our optimized protocol to study its effect on *S. aureus* bacterial membranes. Without any peptide, *S. aureus* was characterized by an M_2 of $22 \times 10^{9}s^{-2}$. With increasing DA6 concentration, M_2 decreased *monotonically* down to a very low value of $3.7 \times 10^{9}s^{-2}$ and reaching the MBC_{HD} at 16 µM (Fig. 3), with a decreasing slope one order of magnitude higher than that of caerin or aurein.

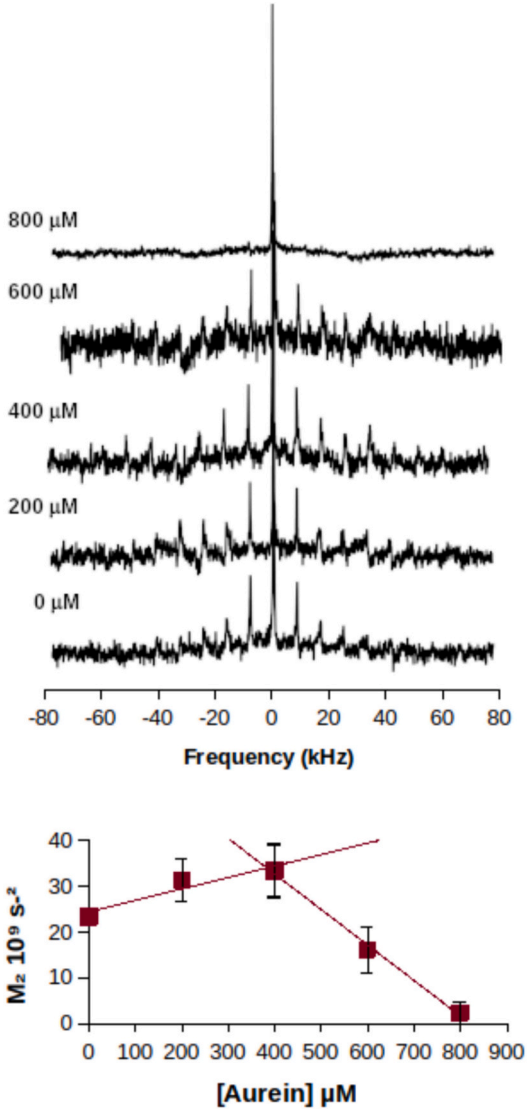

Fig. 2. (top) ^{2}H *in vivo* solid-state NMR spectra of deuterated *S. aureus* with various concentrations of aurein (the central peak is truncated). (bottom) M_2 as a function of aurein concentration, representing the activity curve of aurein on *S. aureus*. All spectra were processed using a 100 Hz exponential multiplication. Each measurement has been repeated three times. The slope of the increasing fitting line is $2.5 \times 10^{7}s^{-2}.\mu M^{-1}$, while that of the decreasing fitting line is $-7.7 \times 10^{7}s^{-2}.\mu M^{-1}$, with an intercept at $MBC_{HD} = 850$ µM.

4. Discussion

4.1. Caerin and aurein

As reported by Laadhari et al. [3] for *B. subtilis*, we observed that increasing concentrations of caerin lead to a linear decrease in M_2 values. This trend is attributed to the progressive formation of membrane pores, each of which reduces membrane order. As the number of pores increases, the integrity of the entire membrane – and consequently the cell - is ultimately compromised. The slope of the activity curve effectively represents a titration of pores within the membrane, which is proportional to the peptide concentration and accounts for the observed linear relationship. As expected, the minimum bactericidal concentration at OD = 12 is an order of magnitude higher than the MBC at OD = 0.003.

Similarly, and in agreement with Laadhari et al. [3] for *B. subtilis*, we found that increasing concentrations of aurein result in a more complex

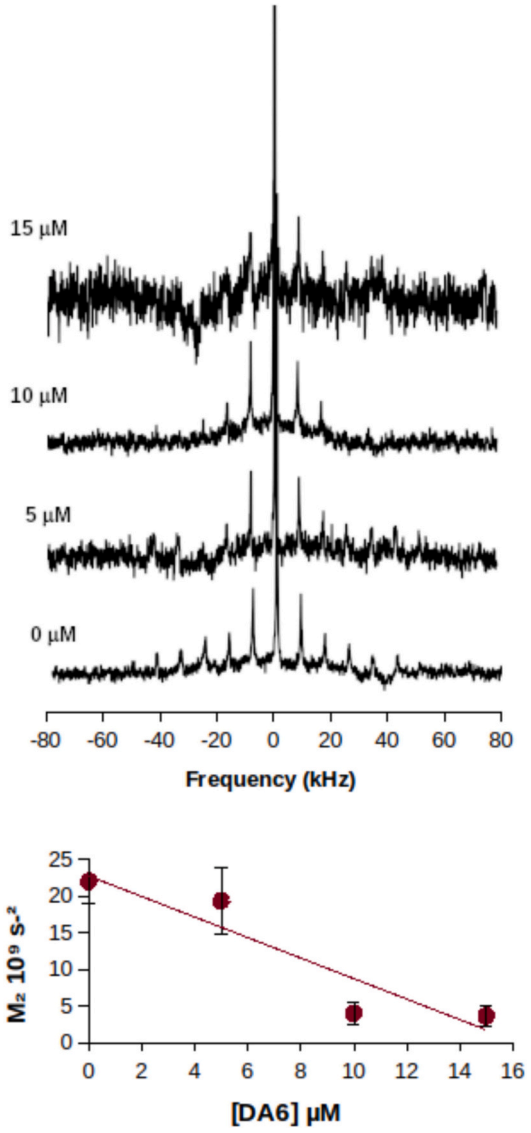

Fig. 3. (top) ^{2}H *in vivo* solid-state NMR spectra of deuterated *S. aureus* with various concentrations of DA6 (the central peak is truncated). (bottom) M_2 as a function of DA6 concentration, representing the activity curve of DA6 on *S. aureus*. All spectra were processed using a 100 Hz exponential multiplication. Each measurement has been repeated three times. The slope of the fitting line is $-1.4 \times 10^{9} s^{-2}.\mu M^{-1}$, with an intercept at $MBC_{HD} = 16$ µM.

response. At low concentrations (relative to the MBC at this high bacterial density), M_2 increases modestly (by *ca.* 40 %). This phenomenon is interpreted as the initial stage of the carpet mechanism, wherein peptides adsorb onto the membrane surface, forming a "carpet", and binding to lipid headgroups, thereby increasing membrane order. At higher concentrations, once the membrane is saturated, the second stage of the carpet mechanism is triggered: rapid micellisation of the entire membrane, the destruction of the cell, and a marked decrease in M_2 values. Note that aurein is shorter than the other two peptides, and more water-soluble. This lower affinity for membranes may also contribute to its higher inhibitory and bactericidal concentrations.

In theory, a similar increase in M_2 should also be observable with caerin, since pore formation is believed to be preceded by peptide binding to lipid headgroups. However, this increase has not been detected, possibly because it occurs within a very narrow concentration range, above which pore forming dominates. For aurein, as anticipated, the slope corresponding to micellisation is much steeper than the initial binding slope, and also exceeds the pore-forming slope observed for caerin. Micellisation is not instantaneous, as not all cells are affected simultaneously. Consequently, the slope reflects more complex behaviors, such as the partitioning of peptides between the solution, the membrane surface or cell wall, and the membrane core.

4.2. DA6

In our study, we observed that in *S. aureus*, increasing concentrations of DA6 result in linear decrease in M_2 values. This behavior closely mirrors that of caerin, and can therefore be interpreted as the formation of an increasing number of DA6-induced pores in the *S. aureus* membrane, elucidating the mechanism of action for this peptide. Although the descending slope of this activity curve likely reflects pore formation by DA6, it is notably steeper than that observed for caerin, This suggests, as previously noted, that the slope is not solely a titration of peptide incorporation into the membrane, and that additional factors are likely involved. The minimum bactericidal concentration for *S. aureus* at OD = 12 is one order of magnitude higher than at OD = 0.003, yet it remains an order of magnitude lower than the MBCs for aurein or caerin. This makes DA6 a promising antimicrobial peptide, even at high bacterial densities, and thus compatible with clinical applications.

The secondary structure, size, hydrophobicity and charge of DA6 are similar to those of caerin. Its length when folded as an α-helix approximates the thickness of a membrane, supporting its classification as a pore-forming peptide [25]. The positive charges on DA6 may facilitate interactions with the negatively charged teichoic acids and lipids on the *S. aureus* surface. However, these similarities do not explain why DA6 is markedly more efficient than caerin. It also does not explain why, despite its higher efficacy, it acts more slowly, with a TK99 that is three times longer than that of caerin. As our understanding of AMP mechanisms advances, new questions continue to arise.

While the solid-state NMR approach described here provides valuable insights into the membrane activity of AMPs, it does not reveal the fate of these peptides prior to membrane disruption. A common feature among these peptides is that they are unstructured in the extracellular environment, but adopt a defined secondary structure upon membrane interaction. The time required for each peptide to adopt this structure may vary. For pore-forming peptides, differences in partition coefficients within the bacterial membrane may influence the kinetics of pore assembly. Furthermore, the number and nature of pores formed (*e.g.*, toroidal, barrel-stave, pore size, and number of peptide monomers per pore) may also affect the peptide-to-lipid ratio, and the time required for pore formation.

Additionally, in *S. aureus*, peptides must cross the cell wall – composed of peptidoglycan and charged teichoic acids - before reaching the membrane, which may involve time-consuming interactions. One possible explanation for our observations is that DA6 interacts strongly with the cell wall or requires more time to adopt a helical structure (long TK99), but subsequently forms pores with fewer monomers (low MBC). In contrast, aurein and caerin may cross the cell wall and adopt a helical structure more rapidly (shorter TK99), but require a higher number of monomers to disrupt the membrane (higher MBC). To address these crucial questions, we are investigating the relatively unexplored process of peptide-cell wall interactions, in collaboration with the laboratory of Isabelle Marcotte at UQAM in Canada (Sandeep et al. in preparation).

5. Conclusion

This study introduces a novel *in vivo* ^{2}H solid-state NMR protocol for investigating the activity of three peptides on *S. aureus*, confirming the mechanism of two peptides, and elucidating the mechanism of a third. This protocol enables the generation of a peptide activity curve within a single day, using a single bacterial culture, thereby improving reproducibility. Moreover, it is readily adaptable to other types of molecules or micro-organisms, including yeasts, fungi, micro-algae or hemocytes.

While we have established that DA6 functions as likely a lytic, pore-

forming antimicrobial peptide, we have not yet determined whether it forms straight or toroidal pores. Recent advances suggest that *in vivo* ^{31}P solid-state NMR could be employed to distinguish between these pore architectures [9]. Much information can also be gathered in future studies by *in vivo* fluorescence microscopy [26,27], molecular dynamic simulations [28], or by performing solid-state NMR experiments on model membranes. With unlabeled peptides, one can determine pore topology or peptide-lipid preferential interactions by ^{31}P NMR [9,29]. Additional studies can also make use of ^{13}C-, ^{15}N- or ^{19}F-labeled peptides, in order to determine peptide orientation and location in the membrane [30,31].

DA6 emerges as a promising drug candidate, due its low cytotoxicity [12], and exceptionally low MBC against Gram(+) bacteria, particularly in comparison to aurein and caerin. In the pursuit of antibiotic alternatives, there is a parallel effort to identify molecules that selectively target pathogenic bacteria while sparing probiotics and other non-pathogenic cells. However, the molecular determinants of such specificity remain poorly understood. Notably, DA6 demonstrates greater activity against *S. aureus* than *E. coli* [12], especially at high bacterial densities that approximate pathogenic conditions (unpublished data), positioning it as a valuable model for investigating bacterial specificity. One promising approach involves detailed analysis of amino-acid sequences, that may explain such behavior, a strategy increasingly facilitated by artificial intelligence for the discovery and optimization of new antimicrobial peptides [32]. Another avenue is the study of specific interaction of this peptide with the *S. aureus* cell wall, an area we are actively exploring (Sandeep et al. in preparation).

While we have optimized a protocol to study peptide interactions with membrane lipids, our future work aims to extend these investigations to other membrane components, such as membrane proteins and cell wall constituents (peptidoglycan, wall teichoic acid, lipoteichoic acid). Although elucidating the precise mode of action of a potential drug is essential for patent applications, our broader objective is to deepen our molecular-level understanding of peptide–cell interactions.

CRediT authorship contribution statement

Laila Zaatouf: Methodology, Investigation, Conceptualization. **Thierry Drujon:** Supervision, Methodology, Investigation. **Astrid Walrant:** Writing – review & editing, Resources. **Emmanuelle Sachon:** Writing – review & editing, Resources. **Dror E. Warschawski:** Writing – review & editing, Writing – original draft, Validation, Supervision, Project administration, Methodology, Investigation, Funding acquisition, Conceptualization.

Funding

LZ was supported by a Ph. D. grant from Sorbonne Université. This work was supported by the Centre National de la Recherche Scientifique (UMR7203), and the Agence Nationale de la Recherche (ANTARBioTic).

Declaration of competing interest

The authors declare that they have no known competing financial interests or personal relationships that could have appeared to influence the work reported in this paper.

Acknowledgments

We thank Claire Lacombe and Marine Cosset who were involved in the early stages of the project. We thank Christophe Piesse for peptide synthesis, and Isabelle Marcotte for helpful discussions.

Appendix A. Supplementary data

Supplementary data to this article can be found online at https://doi.org/10.1016/j.bpc.2025.107532.

Data availability

All the relevant data are contained within this manuscript and supporting information. Source data can be obtained from the corresponding author upon reasonable request.

References

[1] J. Pius, M.R. Morrow, V. Booth, 2H solid-state NMR investigation of whole *Escherichia coli* interacting with antimicrobial peptide MSI-78, Biochemistry 51 (2012) 118–125, https://doi.org/10.1021/bi201569t.
[2] C. Tardy-Laporte, A.A. Arnold, B. Genard, R. Gastineau, M. Morançais, J.L. Mouget, R. Tremblay, I. Marcotte, A 2H solid-state NMR study of the effect of antimicrobial agents on intact *Escherichia coli* without mutating, Biochim. Biophys. Acta 2013 (1828) 614–622, https://doi.org/10.1016/j.bbamem.2012.09.011.
[3] M. Laadhari, A.A. Arnold, A.E. Gravel, F. Separovic, I. Marcotte, Interaction of the antimicrobial peptides caerin 1.1 and aurein 1.2 with intact bacteria by 2H solid-state NMR, Biochim. Biophys. Acta 1858 (2016) 2959–2964, https://doi.org/10.1016/j.bbamem.2016.09.009.
[4] M.-A. Sani, S. Carne, S.A. Overall, A. Poulhazan, F. Separovic, One pathogen two stones: Are Australian tree frog antimicrobial peptides synergistic against human pathogens? Eur. Biophys. J. 46 (2017) 639–646, https://doi.org/10.1007/s00249-017-1215-9.
[5] V. Booth, D.E. Warschawski, N.P. Santisteban, M. Laadhari, I. Marcotte, Recent progress on the application of 2H solid-state NMR to probe the interaction of antimicrobial peptides with intact bacteria, Biochim. Biophys. Acta 1865 (2017) 1500e1511, https://doi.org/10.1016/j.bbapap.2017.07.018.
[6] S.A. Overall, S. Zhu, E. Hanssen, F. Separovic, M.-A. Sani, In situ monitoring of Bacteria under antimicrobial stress using 31P solid-state NMR, Int. J. Mol. Sci. 20 (2019) 181, https://doi.org/10.3390/ijms20010181.
[7] V. Booth, Deuterium solid state NMR studies of intact bacteria treated with antimicrobial peptides, Front. Med. Technol. 2 (2021) 621572, https://doi.org/10.3389/fmedt.2020.621572.
[8] S. Kumari, V. Booth, Antimicrobial peptide mechanisms studied by whole-cell deuterium NMR, Int. J. Mol. Sci. 23 (2022) 2740, https://doi.org/10.3390/ijms23052740.
[9] K. Kumar, M. Sebastiao, A.A. Arnold, S. Bourgault, D.E. Warschawski, I. Marcotte, In situ solid-state NMR study of antimicrobial peptide interactions with erythrocyte membranes, Biophys. J. 121 (2022) 1512e1524, https://doi.org/10.1016/j.bpj.2022.03.009.
[10] K. Kumar, A.A. Arnold, R. Gauthier, M. Mamone, J.-F. Paquin, D.E. Warschawski, I. Marcotte, 19F solid-state NMR approaches to probe antimicrobial peptide interactions with membranes in whole cells, Biochim. Biophys. Acta Biomembr. 1866 (2024) 184269, https://doi.org/10.1016/j.bbamem.2023.184269.
[11] M.-A. Sani, S. Rajput, D.W. Keizer, F. Separovic, NMR techniques for investigating antimicrobial peptides in model membranes and bacterial cells, Methods 224 (2024) 10–20, https://doi.org/10.1016/j.ymeth.2024.01.012.
[12] S. Cardon, E. Sachon, L. Carlier, T. Drujon, A. Walrant, E. Alemán-Navarro, V. Martinez-Osorio, D. Guianvarc'h, S. Sagan, Y. Fleury, R. Marquant, C. Piesse, Y. Rosenstein, C. Auvynet, C. Lacombe, Peptidoglycan potentiates the membrane disrupting effect of the carboxyamidated form of DMS-DA6, a Gram-positive selective antimicrobial peptide isolated from *Pachymedusa dacnicolor* skin, PLoS One 13 (2018) e0205727, https://doi.org/10.1371/journal.pone.0205727.
[13] F. Laydevant, M. Mahabadi, P. Llido, J.-P. Bourgouin, L. Caron, A.A. Arnold, I. Marcotte, D.E. Warschawski, Growth-phase dependence of bacterial membrane lipid profile and labeling for in-cell solid-state NMR applications, Biochim. Biophys. Acta 1864 (2022) 183819, https://doi.org/10.1016/j.bbamem.2021.183819.
[14] L. Zaatouf, K. Kumar, I. Marcotte, D.E. Warschawski, Assessment of membrane labelling mechanisms with exogenous fatty acids and detergents in bacteria, Biochimie 227 (2024) 12e18, https://doi.org/10.1016/j.biochi.2024.05.024.
[15] C. Lacombe, E. Aleman-Navaro, T. Drujon, V. Martinez-Osorio, E. Sachon, E. Melchy-Pérez, L. Carlier, L.E. Fajardo Brigido, Y. Fleury, C. Piesse, G. Gutiérrez-Escobedo, A. De las Peñas, I. Castaño, F. Desriac, J.-L. Beristain-Hernandez, C. Combadiere, Y. Rosenstein, C. Auvynet, Characterization of a new immunosuppressive and antimicrobial peptide, DRS-DA2, isolated from the Mexican frog, Pachymedusa dacnicolor, Int. J. Inf. Secur. 2024 (2024) 2205864, https://doi.org/10.1155/2024/2205864.
[16] X.L. Warnet, M. Laadhari, A.A. Arnold, I. Marcotte, D.E. Warschawski, A 2H magic-angle spinning solid-state NMR characterisation of lipid membranes in intact bacteria, Biochim. Biophys. Acta 2016 (1858) 146–152, https://doi.org/10.1016/j.bbamem.2015.10.020.
[17] C. König, H.-P. Simmen, J. Blaser, Bacterial concentrations in pus and infected peritoneal fluid - implications for bactericidal activity of antibiotics, J. Antimicrob. Chemother. 42 (1998) 227–232, https://doi.org/10.1093/jac/42.2.227.
[18] M. Pullambhatla, J. Tessier, G. Beck, B. Jedynak, J.U. Wurthner, M.G. Pomper, [125I]FIAU imaging in a preclinical model of lung infection: quantification of

bacterial load, Am. J. Nucl. Med. Mol. Imag. 2 (2012) 260–270. https://pmc.ncbi.nlm.nih.gov/articles/PMC3477740/.
[19] A.K. Jepson, J. Schwarz-Linek, L. Ryan, M.G. Ryadnov, W.C.K. Poon, What is the 'minimum inhibitory concentration' (MIC) of Pexiganan acting on *Escherichia coli*? A cautionary case study, Adv. Exp. Med. Biol. 915 (2016) 33–48, https://doi.org/10.1007/978-3-319-32189-9_4.
[20] F. Savini, V. Luca, A. Bocedi, R. Massoud, Y. Park, M.L. Mangoni, L. Stella, Cell-density dependence of host-defense peptide activity and selectivity in the presence of host cells, ACS Chem. Biol. 12 (2017) 52–56, https://doi.org/10.1021/acschembio.6b00910.
[21] K.M. Craft, J.M. Nguyen, L.J. Berg, S.D. Townsend, Methicillin-resistant Staphylococcus aureus (MRSA): antibiotic-resistance and the biofilm phenotype, Medchemcomm 10 (2019) 1231–1241, https://doi.org/10.1039/c9md00044e.
[22] L. Marx, E.F. Semeraro, J. Mandl, J. Kremser, M.P. Frewein, N. Malanovic, K. Lohner, G. Pabst, Bridging the antimicrobial activity of two Lactoferricin derivatives in *E. coli* and lipid-only membranes, Front. Med. Technol. 3 (2021) 625975, https://doi.org/10.3389/fmedt.2021.625975.
[23] D. Roversi, V. Luca, S. Aureli, Y. Park, M.L. Mangoni, L. Stella, How many antimicrobial peptide molecules kill a bacterium? The case of PMAP-23, ACS Chem. Biol. 9 (2014) 2003–2007, https://doi.org/10.1021/cb500426r.
[24] J.H. Davis, Deuterium magnetic resonance study of the gel and liquid crystalline phases of dipalmitoyl phosphatidylcholine, Biophys. J. 27 (1979) 339–358, https://doi.org/10.1016/S0006-3495(79)85222-4.
[25] K.A. Brogden, Antimicrobial peptides: pore formers or metabolic inhibitors in bacteria? Nat. Rev. Microbiol. 3 (2005) 238–250, https://doi.org/10.1038/nrmicro1098.
[26] F. Illien, N. Rodriguez, M. Amoura, A. Joliot, M. Pallerla, S. Cribier, F. Burlina, S. Sagan, Quantitative fluorescence spectroscopy and flow cytometry analyses of cell-penetrating peptides internalization pathways: optimization, pitfalls, comparison with mass spectrometry quantification, Sci. Rep. 6 (2016) 36938, https://doi.org/10.1038/srep36938.
[27] C. Landon, Y. Zhu, M. Mustafi, J.-B. Madinier, D. Lelièvre, V. Aucagne, A. F. Delmas, J.C. Weisshaar, Real-time fluorescence microscopy on Living *E. coli* sheds new light on the antibacterial effects of the king penguin β-Defensin AvBD103b, Int. J. Mol. Sci. 23 (2022) 2057, https://doi.org/10.3390/ijms23042057.
[28] J.D. Richardson, R.C. Van Lehn, Free energy analysis of peptide-induced pore formation in lipid membranes by bridging atomistic and coarse-grained simulations, J. Phys. Chem. B 128 (2024) 8737–8752, https://doi.org/10.1021/acs.jpcb.4c03276.
[29] D.E. Warschawski, A.A. Arnold, I. Marcotte, A new method of assessing lipid mixtures by 31P magic-angle spinning NMR, Biophys. J. 114 (2018) 1368–1376, https://doi.org/10.1016/j.bpj.2018.01.025.
[30] N.S. Shu, M.S. Chung, L. Yao, M. An, W. Qiang, Residue-specific structures and membrane locations of pH-low insertion peptide by solid-state nuclear magnetic resonance, Nat. Commun. 6 (2015) 7787, https://doi.org/10.1038/ncomms8787.
[31] S.L. Grage, M.-A. Sani, O. Cheneval, S.T. Henriques, C. Schalck, R. Heinzmann, J. S. Mylne, P.K. Mykhailiuk, S. Afonin, I.V. Komarov, F. Separovic, D.J. Craik, A. S. Ulrich, Orientation and location of the Cyclotide Kalata B1 in lipid bilayers revealed by solid-state NMR, Biophys. J. 112 (2017) 630–642, https://doi.org/10.1016/j.bpj.2016.12.040.
[32] P. Szymczak, E. Szczurek, Artificial intelligence-driven antimicrobial peptide discovery, Curr. Opin. Struct. Biol. 83 (2023) 102733, https://doi.org/10.1016/j.sbi.2023.102733.

Antimicrobial peptide mechanism of action on *S. aureus* membranes determined by *in vivo* solid-state NMR

Laila ZAATOUF, Thierry DRUJON, Astrid WALRANT, Emmanuelle SACHON, and Dror E. WARSCHAWSKI*

Chimie Physique et Chimie du Vivant, CPCV, CNRS UMR 8228, Sorbonne Université, École normale supérieure, PSL University, 75005 Paris, France

Corresponding author: Dror WARSCHAWSKI, dror.warschawski@sorbonne-universite.fr

Supplementary Material

Table S1. Antimicrobial peptide concentrations used (μM)

AMP	**for *S. aureus***
aurein	0, 200, 400, 600, 800
caerin	0, 200, 400, 600
DA6	0, 5, 10, 15

Lipid profile

Table S2. Phospholipid headgroup proportions in *S. aureus*, with or without 50 mM exogenous PA-d_{31}, micellized in Tween 20, determined by ^{31}P solution NMR.

Phospholipid headgroup	Native	With PA-d_{31}
PG	82	73
CL	4	5
LPG	14	22

Table S3. Fatty acid proportions in *S. aureus*, with or without 50 mM exogenous PA-d_{31}, micellized in Tween 20, determined by GCMS.

Fatty acid	Native	With PA-d_{31}
Iso-C15:0	7	1
Anteiso-C15:0	57	29
C16:0 (PA)	1	6
C16:0-d_{31} (PA-d_{31})	X	38
Iso-C17:0	4	< 1
Anteiso-C17:0	12	< 1
C18:0	5	10
Iso-C19:0	4	4
Anteiso-C19:0	3	0
C20:0	6	10

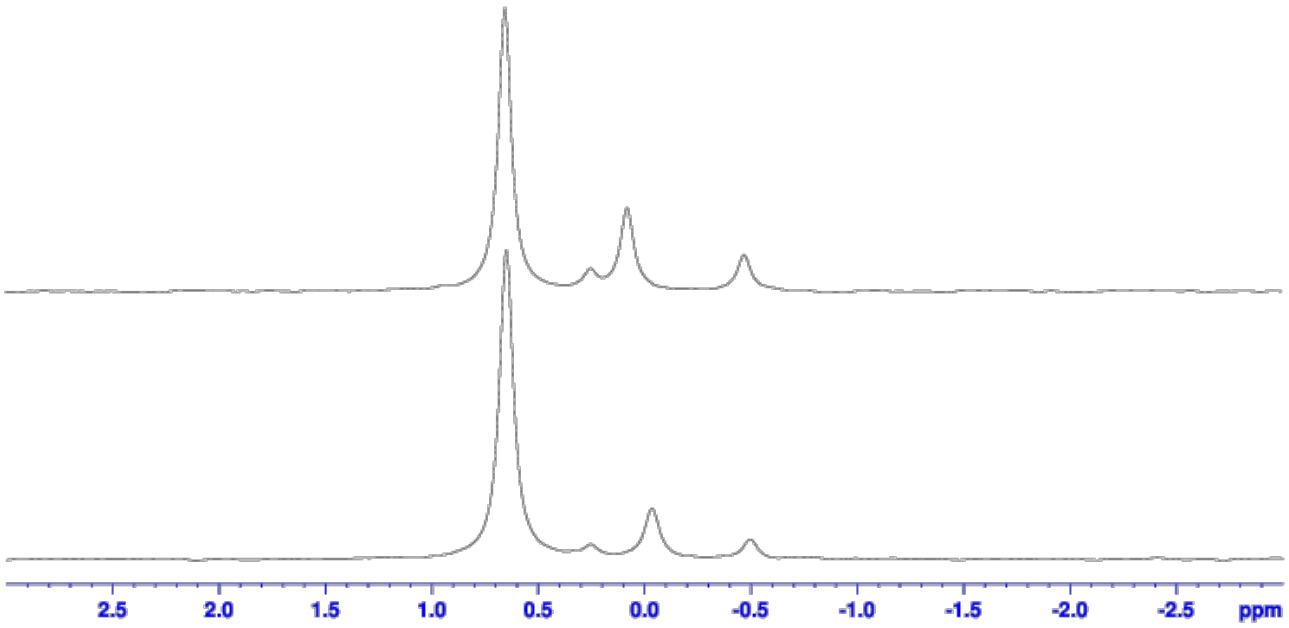

Figure S1: ^{31}P solution NMR of *S. aureus* phospholipids with (top) and without (bottom) 50 μM exogenous PA-d_{31} micellized in Tween 20